Langmuir

Letter

pubs.acs.org/Langmuir

Rhodium(0) Nanoparticles Supported on Nanocrystalline Hydroxyapatite: Highly Effective Catalytic System for the Solvent-Free Hydrogenation of Aromatics at Room Temperature

Mehmet Zahmakıran,[†,§] Yuriy Román-Leshkov,*[,†,§] and Yong Zhang[‡,§]

[†]Department of Chemical Engineering and [‡]Center for Materials Science and Engineering, Massachusetts Institute of Technology, Cambridge, Massachusetts 02139, United States

Supporting Information

ABSTRACT: The hydrogenation of aromatics under mild conditions remains a challenge in the fields of synthetic and petroleum chemistry. Described herein is a new catalytic material that shows excellent catalytic performance in terms of activity, selectivity, and reusability in the hydrogenation of aromatics in solvent-free systems under mild conditions. The catalyst, consisting of rhodium nanoparticles supported on nanocrystalline hydroxyapatite, can quantitatively hydrogenate neat benzene to cyclohexane with exceptionally high rates (initial TOF > 10^3 h^{-1}) at 298 K and 3 bars of initial H_2 pressure. This new material maintains its inherent catalytic activity after several reuses. Importantly, catalyst preparation does not require elaborate procedures because the active metal nanoparticles are readily formed from the in situ reduction of Rh^{3+}-exchanged hydroxyapatite while submerged in the aromatic solvent at room temperature under 3 bars of H_2 pressure.

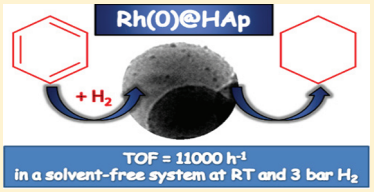

INTRODUCTION

The hydrogenation of aromatic molecules is an important reaction in the petroleum and chemical industries. For instance, cyclohexane obtained from the complete hydrogenation of benzene is a high-volume intermediate used in the production of Nylon 6.[1] New regulations call for a drastic reduction in the aromatic content in fuels because these molecules have been shown to be highly detrimental toward both fuel quality and human health.[2] Most studies regarding aromatic hydrogenation have used benzene as the model aromatic feed molecule, and transition-metal nanoparticles and organometallic complexes have been thoroughly investigated as catalysts for the saturation of its C=C bonds.[3,4] Indeed, benzene is notoriously difficult to hydrogenate when compared to olefins because of the resonance stabilization imparted by the aromatic ring. Thus, hydrogenation reaction conditions often require temperatures >373 K, H_2 pressures >30 bar, and/or dilution of the aromatic substrate with a solvent, leading to higher byproduct generation and more energy-intensive product separation procedures. Very few reports exist on catalytic schemes that perform the complete hydrogenation of benzene under mild conditions (i.e., ≤300 K and <10 bars of H_2) and under solvent-free conditions with acceptable rates. Unfortunately, most of the catalysts used in these schemes suffer from either low activity,[3a,d] low stability,[3a,b,i] or difficult[3b−d,g] and time-consuming[3c−h] synthesis procedures (Table S-1 in the Supporting Information). Therefore, the development of a simply prepared, highly active, reusable catalyst that operates under mild and solvent-free conditions remains a difficult challenge in the hydrogenation of aromatics.[5]

Recently, hydroxyapatite ($[Ca_{10}(OH)_2(PO_4)_6]$, HAp)[6] has generated great interest in view of its potential application in a wide variety of fields,[7] including in catalysis as a support with attractive properties.[8] Specifically, HAp has the following advantages as a catalyst support: (i) reduced mass transfer limitations due to the absence of structural porosity, (ii) a high ion-exchange ability and adsorption capacity, and (iii) a low surface acidity, thus preventing any side reactions arising from the support itself.[8] These physicochemical properties of HAp prompted us to focus on the use of the HAp matrix in the stabilization of metal nanoparticles. The reduction of the HAp matrix particle size from the microcrystalline to the nanocrystalline regime (from >1 μm to <100 nm) was performed in anticipation of improved activity due to a higher external surface area, a larger number of exchange sites, and lower mass-transfer limitations for liquid-phase hydrogenation at low temperature.

In this letter, we report our results on the preparation and characterization of a catalyst consisting of rhodium(0) nanoparticles (2.7 ± 1.1 nm) supported on a nanocrystalline (80 ± 15 nm) HAp matrix, hereafter referred to as Rh(0)@HAp, and on its remarkable catalytic performance in terms of the activity, selectivity, and reusability in the hydrogenation of aromatics in solvent-free systems under mild conditions. Rh@HAp can be reproducibly prepared with exceptional simplicity by the ion exchange[9] of Rh^{3+} ions with Ca^{2+} ions of the HAp matrix, followed by the reduction of Rh^{3+}-exchanged nanocrystalline hydroxyapatite (Rh^{3+}@HAp) in situ during the hydrogenation of an aromatic substrate. After an induction period, the resulting Rh(0)@HAp hydrogenates aromatic

Received: November 9, 2011
Revised: December 5, 2011
Published: December 6, 2011

 © 2011 American Chemical Society dx.doi.org/10.1021/la2044174 | *Langmuir* 2012, 28, 60−64

substrates (e.g., benzene, toluene, *m*-xylene, *o*-xylene, and *p*-xylene) to their corresponding saturated alkanes at high rates under solvent-free, mild conditions (at 298 K and under 3 bars of initial H_2 pressure). More importantly, the supported rhodium(0) nanoparticles on the HAp matrix feature notable resistance against agglomeration and leaching. Indeed, when the isolated Rh@Hap catalyst is reused, it retains 92% of its initial catalytic activity after five cycles of quantitative hydrogenation of neat benzene into cyclohexane under the same reaction conditions.

EXPERIMENTAL SECTION

Materials. Synthetic hydroxyapatite nanocrystalline powder ($[Ca_5(OH)(PO_4)_3]_x$, ≥99.995% trace metals basis), hydroxyapatite powder ($[Ca_5(OH)(PO_4)_3]_x$), benzene (Chromasolv Plus, for HPLC, ≥99%), toluene (anhydrous, ≥99.8%), *m*-xylene (anhydrous, ≥99%), *o*-xylene (anhydrous, ≥99%), *p*-xylene (anhydrous, ≥99%), cyclohexene (puriss. p.a., ≥99.5%), and carbon disulfide (CS_2, anhydrous, ≥99%) were purchased from Sigma-Aldrich and used as received. Rhodium(III) chloride trihydrate ($RhCl_3{\cdot}3H_2O$) and *d*-chloroform ($CDCl_3$) were purchased from Strem Chemicals and Cambridge Isotope Laboratories, respectively. Deionized water was distilled with a water purification system (Thermo Scientific Barnsted Nanopure System). All glassware and Teflon-coated magnetic stir bars were cleaned with acetone, followed by copious rinsing with doubly deionized water under ultrasonication, and finally dried in an oven at 423 K.

Preparation of Rh^{3+}@HAp and General Procedure for the In Situ Generation of Rh(0)@HAp During the Hydrogenation of Aromatics. Rhodium(III) cations were introduced into Ca^{2+}@HAp by the ion exchange of 500 mg of Ca^{2+}@HAp in 20 mL of an aqueous solution of 25.3 mg of $RhCl_3{\cdot}3H_2O$ (0.09 mmol) for 4 h at room temperature. The sample was then filtered by suction filtration using a Whatman-1 filter (Ø = 9 cm), washed three times with 100 mL of deionized water, and dried at 353 K in the oven. The in situ formation of Rh(0)@HAp and the concomitant hydrogenation of olefinic or aromatic substrates were performed in a Fischer–Porter (F–P) pressure bottle connected to a line through Swagelock tetrafluoroethylene (TFE)-sealed quick connects and to an Omega-PX209-100GI pressure transducer interfaced through an Omega-UWPC-2-NEMA wireless transmitter to a computer using an Omega-UWTC-REC2-D-V2 wireless receiver. The progress of an individual hydrogenation reaction was followed by monitoring the pressure of H_2 gas on the Omega-data logging and using the recording software program. In a typical experiment, 100 mg of Rh^{3+}@HAp (4.86 μmol Rh) was weighted and placed in a new 22 × 175 mm pyrex culture tube containing a new $^5/_{16}$ in. × $^5/_8$ in. stir bar. The culture tube was then placed inside the F–P bottle, and the entire setup was placed inside a constant-temperature circulating water bath thermostatted at 298 K and purged/evacuated for at least 30 min to remove any trace of oxygen and water. Next, 1 mL of substrate was added to the F–P bottle rapidly via a syringe with a long needle under hydrogen purging. Afterward, the bottle was purged 10 times with H_2 (15 s per purge with stirring at 1000 rpm), and the reaction timer was started (t = 0 min). When no more hydrogen uptake was observed, the experiment was stopped, the F–P bottle was closed and disconnected from the line, and the hydrogen pressure was released. Finally, a small aliquot from the reaction solution in the culture tube was withdrawn for ^{1}H NMR analysis.

Data Handling and Curve Fit of Hydrogenation Data. The raw pressure versus time data collected with the computer-interfaced transducer were exported from Omega software program and imported into OriginPro 8, which was then converted into the equivalent concentration loss of substrate using the known stoichiometry (for example; 3:1 for H_2/C_6H_6 in the complete hydrogenation of benzene). The curve fitting of the [substrate] versus time data to the Finke–Watzky two-step mechanism was performed as described elsewhere[10] using the software package OriginPro 8, which is a nonlinear regression subroutine and uses a modified Levenberg–Marquardt algorithm.

RESULTS AND DISCUSSION

The progress of Rh(0)@HAp formation and the concomitant hydrogenation of neat aromatics at room temperature were followed by monitoring changes in the hydrogen pressure and converting them into an equivalent substrate concentration loss using known hydrogenation stoichiometries (e.g., 3:1 H_2/substrate for the complete hydrogenation of benzene). As observed in Figure 1, the hydrogenation of neat benzene

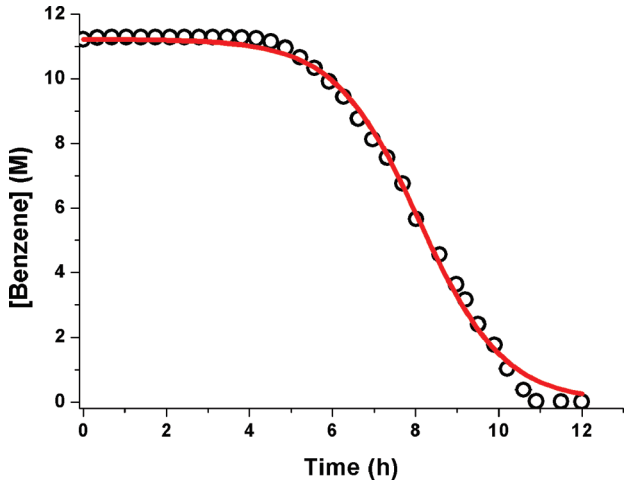

Figure 1. Plot of benzene concentration vs time for the hydrogenation of 1 mL of benzene (11.2 mmol) starting with 100 mg of Rh^{3+}@HAp (0.5 wt % loading, corresponding to 0.00486 mmol of Rh) at 298 K and an initial H_2 pressure of 3 bars in a batch reactor. Circles correspond to experimental data, and the solid line represents a theoretical curve fit to a hydrogenation sequence occurring on a metal undergoing a Finke–Watzky two-step nanoparticle formation mechanism[10] (k_1 = 0.0036 ± 0.00073 h^{-1} and k_2 = 201.23 ± 5.84 M h^{-1} with R^2 = 0.997).

starting with the Rh^{3+}@HAp precatalyst at 298 K and 3 bars of H_2 pressure follows sigmoidal kinetics that fit well with the Finke–Watzky (F–W) two-step nucleation and autocatalytic growth mechanism.[10] The F–W mechanism models the formation of nanoparticles by considering a slow, continuous nucleation step (A → B, rate constant k_1) followed by an autocatalytic surface growth step (A + B → 2B, rate constant k_2) that results in a sigmoidally shaped hydrogenation curve.[7] Thus, the complete hydrogenation of neat benzene catalyzed by Rh(0)@HAp containing 0.5 wt % Rh (as determined by inductively coupled plasma mass spectroscopy [ICP-MS] with 14.1 and 36.8 wt % P and Ca, respectively) was achieved within 5 h after an induction time period of ∼6 h, as judged by the cessation of H_2 uptake and the quantitative producton of cyclohexane (>99% yield confirmed by ^{1}H NMR). The excellent fit to F–W kinetics is indicative of the formation of metal(0) nanoparticles from the ion-exchanged precatalyst in the presence of a reducing agent at room temperature.[11,12] We note that none of the partially hydrogenated benzene reduction products (e.g., cyclohexene) were observed during the reaction. No hydrogenation of benzene was observed when the reaction was carried out using rhodium-free nanocrystalline HAp, indicating that the support is catalytically inactive for this reaction.

dx.doi.org/10.1021/la2044174 | *Langmuir* 2012, 28, 60–64

After the complete hydrogenation of benzene was achieved, the catalyst was isolated by simple filtration and characterized using several analytical techniques. Powder X-ray diffraction (PXRD) patterns of Rh(0)@HAp are identical to that of the host HAp framework (Figure SI-1), thus indicating that no new phases appear after the formation of Rh(0)@HAp and that, after reaction, no observable alterations in the framework lattice or a loss in crystallinity is detected.[13,14] Transmission electron microscopy (TEM) images reveal the presence of Rh(0) nanoparticles on the HAp matrix in the range of 1.0−4.0 nm with a mean diameter of 2.7 ± 1.1 nm, which corresponds to $Rh(0)_{\sim 748}$ nanoclusters (Figure 2).[15] High-resolution TEM

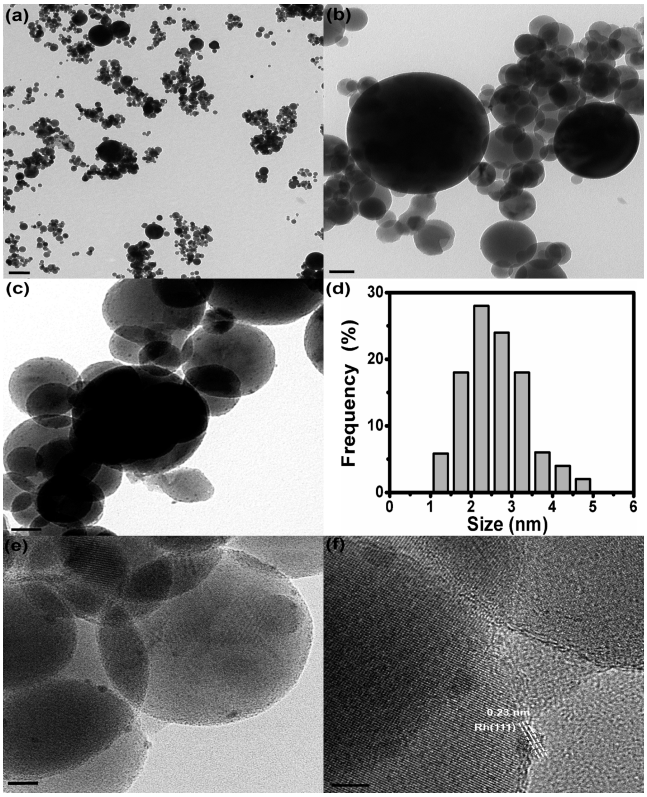

Figure 2. (a−c) TEM images of Rh@HAp for different magnification scale bars equal to 100, 50, and 20 nm, respectively. (d) Size histogram of Rh@HAp. (e, f) High-resolution TEM images of Rh@HAp in which scale bars correspond to 10 and 2 nm, respectively.

images of the supported Rh(0) nanoparticles show an interplanar spacing of ~0.23 nm, conforming to the {111} plane of cubic Rh nanoparticles (Figure 2e).[16] The high-angle annular dark-field scanning TEM (HAADF-STEM) images (Figure 3a−d) of Rh(0)@HAp mapped for Ca, P, and Rh indicate that the Rh(0) nanoparticles are well dispersed throughout the hydroxyapatite matrix. The oxidation state of rhodium and the surface composition of Rh(0)@HAp were investigated by X-ray photoelectron spectroscopy (XPS). The survey-scan XPS spectrum of Rh(0)@HAp (Figure SI-2a) suggests that rhodium is the only element detected in addition to the HAp framework elements (Ca, P, and O). The high-resolution Rh 3d XPS spectrum of Rh(0)@HAp (Figure SI-2b) gives two prominent bands at 308 and 312.4 eV that are readily assigned to Rh(0) $3d_{5/2}$ and Rh(0) $3d_{3/2}$, respectively, thus indicating the complete reduction of Rh(III) on HAp to Rh(0) by H_2 during the hydrogenation of benzene.[17] Compared to the

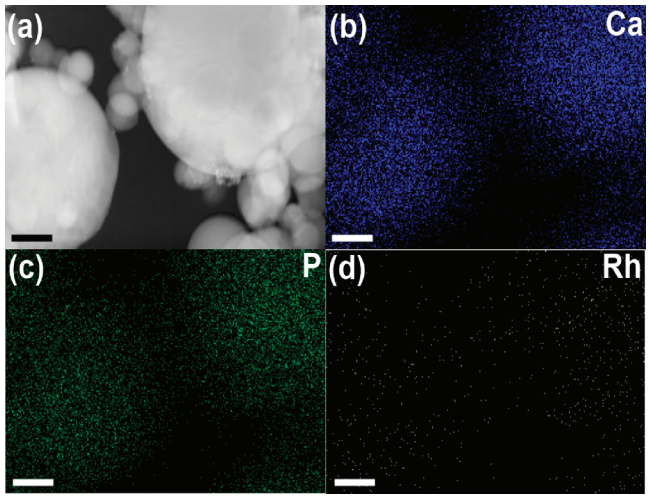

Figure 3. (a)High-angle annular dark-field scanning TEM (HAADF-STEM) image of Rh(0)@HAp and its elemental mapping for (b) Ca, (c) P, and (d) Rh.

value of metallic rhodium 3d peaks, the slight shift (ΔE_b = +0.6 eV) observed in Rh(0)@HAp toward a higher energy value can be attributed to the peculiar electronic properties of the HAp matrix[6,8] and surface oxidation during the XPS sampling procedure.[18] Additionally, the interaction of rhodium(0) nanoparticles with the framework oxygen of the HAp matrix induces a positive charge on the rhodium surface, which would increase the Rh 3d binding energy of rhodium(0) nanoparticles.[18] The N_2 adsorption isotherms of both HAp and Rh(0)@HAp (Figure SI-3) show type III isotherms reflecting the absence of micropores (<2 nm).[19] Surface areas of 19 and 35 $m^2\ g^{-1}$ were calculated for Rh(0)@Hap and the parent HAp, respectively. The reduction in surface area for Rh(0)@Hap is associated with the presence of rhodium nanoparticles on the HAp surface.

Prior to kinetic measurements, the absence of external and internal mass transfer limitations was confirmed by performing the Madon−Boudart test[20,21] and by obtaining a Weisz−Prater (WP) parameter value of ≪0.3, following the methodology suggested by Mukherjee and Vannice.[22] A range of initial turnover frequency (TOF) values was calculated using the number of active surface sites determined through multiple techniques. CO chemisorption experiments on Rh(0)@HAp indicate CO/Rh uptake values of 1.78 ± 0.1. Indeed, surface species in Rh nanoparticles can form both mono- and dicarbonyl complexes with CO, thus explaining CO/Rh uptake values that are greater than 1.[23] Although CO chemisorption values cannot be used to quantify the exact number of surface Rh species, these data suggest that Rh is highly dispersed on the support. Thus, a sensible assumption of a 100% metal dispersion translates into a remarkable lower bound initial TOF for benzene hydrogenation of 1770 h^{-1}. However, different surface sites (i.e., high-coordination-number terrace atoms and low-coordination-number edge and corner atoms) may feature drastically different reactivity profiles. Carbon disulfide (CS_2) poisoning experiments were performed to identify the number of active surface species. Specifically, a series of independent benzene hydrogenation experiments with varying $[CS_2]/[Rh]$ ratios were performed to determine the amount of CS_2 required to deactivate the Rh(0)@HAp catalyst. It was found that 0.032 mol equiv of CS_2 is sufficient to poison

dx.doi.org/10.1021/la2044174 | Langmuir 2012, 28, 60−64

all of the available active Rh sites in the catalyst and completely stop the reaction (Figure SI-4). Coupling this result with a 1:5 CS_2/Rh stoichiometry, as suggested by Hornstein and co-workers based on single-crystal data,[12] results in 16% of the total number of Rh atoms being catalytically available and active for the hydrogenation of benzene. Using this value, an exceptional higher bound initial TOF of 11 000 h^{-1} is obtained. Although the precise CS_2/Rh stoichiometry remains under debate, the poisoning experiments indicate that only a fraction of the surface sites are responsible for catalyzing the hydrogenation reaction. Adopting the model of full-shell nanoparticles[24] for cuboctahedral Rh crystallites allows for the calculation of total (N_T) and surface (N_S) (high-coordination [N_{HS}] and low-coordination [N_{LS}]) atoms using eqs 1−5

$$d_{sph} = 1.105 d_{at} N_T^{1/3} \quad (1)$$

$$N_T = \frac{10m^3 - 15m^2 + 11m - 3}{3} \quad (2)$$

$$N_S = 10m^2 - 20m + 12 \quad (3)$$

$$N_{HS} = 6(m-2)^2 + 4(m-3)(m-2) \quad (4)$$

$$N_{LS} = 24(m-2) + 12 \quad (5)$$

where d_{sph} is the mean diameter of the Rh crystallites obtained from TEM analysis and d_{at} is the atom diameter of Rh (0.268 nm). Thus, it is observed that highly reactive low-coordination-number atoms (N_{LS}) correspond to 16.1% of the total number of Rh atoms for 2.7 nm nanoparticles, which is in good agreement with the results obtained from CS_2 poisoning experiments.

Reusability experiments geared to assessing the stability of Rh(0)@HAp indicated that the catalyst is very robust and does not undergo deactivation after several hydrogenation cycles. After the complete hydrogenation of benzene in the first run, Rh(0)@HAp was isolated as a dark-brown powder by simple filtration and dried under vacuum at room temperature. The Rh(0)@HAp sample can be safely bottled and stored under ambient conditions. Furthermore, when reused, Rh(0)@HAp retains 92% of its initial catalytic activity after five cycles, achieving the complete hydrogenation of benzene in each cycle without jeopardizing the selectivity (Figure 4). This translates into a lower-bound turnover number [TON] of 11 520.[25] The slight decrease in the initial catalytic activity can be attributed to a decrease in the number of active surface atoms due to a small increase in the size of the Rh(0) nanoparticles from 2.7 ± 1.1 nm ($Rh(0)_{\sim 748}$ nanoclusters) to 3.2 ± 0.9 nm ($Rh(0)_{\sim 1245}$ nanoclusters),[15] as measured for Rh(0)@HAp recovered at the end of the first and third cycles, respectively. Importantly, no rhodium leaching was detected in the filtrate solution collected at the end of the reaction (analyzed by ICP-MS with a detection limit of 30 ppb for Rh). A control experiment showed that the hydrogenation of benzene did not continue after Rh(0)@HAp was removed shortly after the reaction had started, confirming no leaching of active catalyst to the solution.

The in situ generation of Rh(0)@HAp and its subsequent use as a hydrogenation catalyst was also demonstrated using various other substrates, including cyclohexene, toluene, *m*-xylene, *o*-xylene, and *p*-xylene (Table 1 and Figures SI-7−SI-11). In all cases, Rh(0)@HAp provided high hydrogenation rates and TOF values[25] with quantitative yields of the corresponding saturated product under solvent-free conditions at 298 K and 3 bars of initial H_2 pressure. As expected, cyclohexene hydrogenation rates are faster when compared to benzene hydrogenation rates because the resonance stabilization energy is typically absent in olefins.[1] Also, slower hydrogenation rates are observed with increasing methyl substituents in the aromatic ring, in agreement with previous reports showing that methyl substituents on the benzene ring act as electron-contributing groups that stabilize π complexation, thereby increasing the energy barrier toward hydrogenation.[26] The observed trend in the hydrogenation rate of xylenes (*p*-xylene > *m*-xylene > *o*-xylene) can be explained by the steric hindrance resulting from the position of the methyl groups that hinder the accessibility of one of the C═C bonds

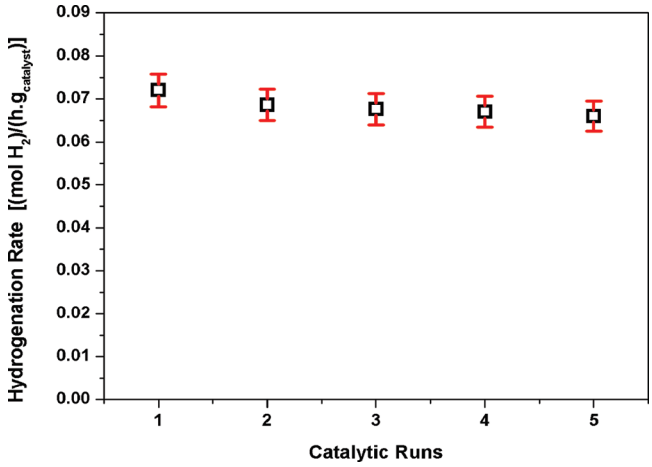

Figure 4. Hydrogenation rate vs catalytic runs determined for the Rh@HAp-catalyzed hydrogenation of benzene at 298 K and an initial 3 bars of H_2 pressure. Initial rates were determined at conversion levels of ≤20%.

Table 1. Hydrogenation of Olefins and Arenes Using Rh(0)@HAp[a]

Entry	Substrate	Product[b]	Initial Hydrogenation Rate[c] [mol H_2 $g_{catalyst}^{-1}h^{-1}$]×10^3	TOF (h^{-1})[c,d]
1			112	2750
2			72	1770
3			40	980
4			7	170
5			13	320
6	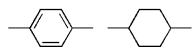		16	395

[a]The reaction conditions are 1 mL of substrate + 100 mg of Rh(0)@HAp with a 0.5 wt % Rh loading (4.86 μmol Rh) at 298 K and 3 bars of initial H_2 pressure. [b]In all tests, >99% conversion and selectivity were obtained. [c]Determined at conversion levels of ≤15%. [d]Reported TOF values are based on the total number of moles of Rh and thus are not corrected for the actual number of surface-active sites.

dx.doi.org/10.1021/la2044174 | *Langmuir* 2012, 28, 60−64

to the active rhodium sites, which is most prominent in the case of *o*-xylene.[27]

CONCLUSIONS

Novel Rh(0)@HAp has been reproducibly prepared from the in situ reduction of Rh^{3+}@HAp in pure olefinic or aromatic substrates. Rh(0)@HAp is a highly active and selective catalyst for the hydrogenation of olefins and arenes under solvent-free, mild reaction conditions (298 K and 3 bars of initial H_2 pressure). This material demonstrates exceptional catalytic activity (TOF = 11 000 h^{-1}) and reusability (92% of inherent activity after the fifth reuse) for the hydrogenation of benzene. Several advanced analytical tools have been used to characterize the material, highlighting the role of the Rh(0) nanoparticles as the active species. Understanding the existing synergistic effects between the metal and HAp support remains an active area of research in our group. High catalytic activity, reusability, and simple preparation and isolation procedures make Rh(0)@HAp a very attractive catalyst for performing selective aromatic hydrogenation reactions.

ASSOCIATED CONTENT

Supporting Information

Includes the experimental procedure, results of the characterization of Rh(0)@Hap, and the hydrogenation of different substrates. This material is available free of charge via the Internet at http://pubs.acs.org.

AUTHOR INFORMATION

Corresponding Author

*E-mail: yroman@mit.edu. Fax: 617-258-5042.

Author Contributions

[§]M.Z. designed and performed the experiments. M.Z. and Y.R.-L. discussed the results and wrote the article. Y.Z. performed TEM, HRTEM, STEM and HAADF-STEM analyses.

ACKNOWLEDGMENTS

M.Z. expresses his gratitude to the Yüzüncü Yıl University for allowing him to conduct his research at MIT. We thank the King Fahd University of Petroleum and Minerals in Dharam, Saudi Arabia, for funding the research reported in this letter through the Center for Clean Water and Clean Energy at MIT and KFUPM. We thank Mark M. Wright for his help in the construction of the reactor setup.

REFERENCES

(1) Larock, R. C. *Comprehensive Organic Transformations*: Wiley-VCH, New York, 1999.
(2) Stanislaus, A.; Cooper, B. H. *Catal. Rev. Sci. Eng.* **1994**, *36*, 75.
(3) (a) Seeberger, M. H.; Jones, R. A. *J. Chem. Soc. Chem. Comm.* **1985**, *6*, 373. (b) Duan, Z.; Sylwester, A. P.; Hampden-Smith, M. J. *Chem. Mater.* **1992**, *4*, 1146. (c) Mevellec, V.; Ramirez, E.; Phillippot, K.; Chaudret, B.; Roucoux, A. *Adv. Synth. Cat.* **2004**, *346*, 72. (d) Zhang, J.; Xie, Z.; Liu, Z.; Wu, W.; Han, B.; Huang, J.; Jiang, T. *Catal. Lett.* **2005**, *103*, 59. (e) Zahmakıran, M.; Özkar, S. *Langmuir* **2008**, *24*, 7065. (f) Pan, H.-B.; Wai, C. M. *J. Phys. Chem. C* **2009**, *113*, 19782. (g) Zahmakıran, M.; Tonbul, Y.; Özkar, S. *J. Am. Chem. Soc.* **2010**, *132*, 6541. (h) Zahmakıran, M.; Tonbul, Y.; Özkar, S. *Chem. Commun.* **2010**, *46*, 4788. (i) Bayram, E.; Zahmakıran, M.; Özkar, S.; Finke, R. G. *Langmuir* **2010**, *46*, 12455. (j) Hwu, H. H.; Eng, J.; Chen, J. G. *J. Am. Chem. Soc.* **2002**, *124*, 702.
(4) Nicholas, J. P.; Ahn, H.; Marks, T. J. *J. Am. Chem. Soc.* **2003**, *125*, 4325.
(5) Poliakoff, M.; Fitzpatrick, J. M.; Farren, T. R.; Anastas, P. T. *Science* **2002**, *297*, 807.
(6) Elliot, J. C. *Structure and Chemistry of Apatites and Other Calcium Orthophosphates*, Elsevier, Amsterdam, 1994.
(7) (a) Palmer, L. C.; Newcomb, C. J.; Kaltz, S. R.; Spoerke, E. D.; Stupp, S. I. *Chem. Rev.* **2008**, *108*, 4754. (b) Mura-Galelli, M. J.; Voegel, J. C.; Behr, S.; Bres, E. F.; Schaaf, P. *Proc. Natl. Acad. Sci.* **1991**, *88*, 5557. (c) Reichert, J.; Binner, J. G. P. *J. Mater. Sci.* **1996**, *31*, 1231.
(8) Kaneda, K.; Mizugaki, T. *Energ. Environ. Sci.* **2009**, *2*, 655 and references cited therein.
(9) Breck, D. W. *Zeolite Molecular Sieves*: Wiley, New York, 1984.
(10) (a) Watzky, M. A.; Finke, R. G. *J. Am. Chem. Soc.* **1997**, *119*, 10382. (b) Mondloch, J. E.; Yan, X.; Finke, R. G. *J. Am. Chem. Soc.* **2009**, *131*, 6389.
(11) Zahmakıran, M.; Özkar, S. *Inorg. Chem.* **2009**, *48*, 8955.
(12) Hornstein, B. J.; Aiken, J. D.; Finke, R. G. *Inorg. Chem.* **2002**, *41*, 1625.
(13) On passing from HAp to Rh(III)@HAp and Rh(0)@HAp the slight shift observed in the PXRD diffraction angles indicates the compression of HAp structure in the presence of Rh^{3+} cations and Rh^0 nanoparticles. Additionally, the introduction of trivalent Rh^{3+} ions to replace divalent Ca^{2+} plus formation of Rh^0 nanoparticles on the surface of HAp may lead to change into some extent in the symmetry of crystalline structure. The similar results were observed in zeolite framework stabilized metal nanoparticles in which host matrix provides framework oxygen interacted cation exchangeable sites, please see; (a) Bouvy, C.; Marine, W.; Sporken, R.; Su, B. L. *Chem. Phys. Lett.* **2006**, *428*, 312. (b) Garcia, M. M.; Villavicencio, H.; Hernández-Vélez, M.; Sánchez, O.; Martínez-Duarta, J. M. *Mater. Sci. Eng: C* **2001**, *15*, 101. (c) Sadjadi, M. S.; Pourahmad, A.; Sohrabnezhad, S.; Zare, K. *Mater. Lett.* **2007**, *61*, 2923.
(14) The decrease in the intensity of Bragg peaks (or the absence of some of them) in Rh(0)@HAp can be explained by the changes in the charge distribution and electrostatic fields as result of (*i*) the existence of Rh(0) nanoparticles on the surface and interaction of their electrophilic surface with framework oxygen atoms, (*ii*) the occupancy of Ca^{2+} ions' sites by H^+ ions (formed the reduction of Rh^{3+} by dihydrogen; $Rh^{3+} + 3/2\ H_2 \rightarrow Rh^0 + 3H^+$) at the end of the formation of Rh(0)@HAp. Nevertheless, most peaks are not changed and do not change after reaction. Additionally, the low resolution-TEM images of HAp taken before and after reduction of Rh^{3+}@HAp show the same crystalline morphology (no agglomeration that can lead to amorphous phase).
(15) Using the equation $N = N_o pV/101.1$, where $N_o = 6.022 \times 10^{23}$, p = 12.4 g cm^{-3} and $V = (4/3)\pi r^3$, the number of metal atoms in spherical 2.7 and 3.2 nm rhodium(0) nanoclusters were estimated to be 748 and 1245, respectively.
(16) Hoefelmeyer, J. D.; Niesz, K.; Somorjai, G. A.; Tilley, T. D. *Nano Lett.* **2005**, *5*, 435.
(17) Mevellec, V.; Nowicki, A.; Roucoux, A.; Dujardin, C.; Granger, P.; Payen, E.; Philippot, K. *New J. Chem.* **2006**, *30*, 1214.
(18) Zahmakıran, M.; Özkar, S. *Langmuir* **2009**, *25*, 2667.
(19) Storck, S.; Bretinger, H.; Maier, W. F. *Appl. Catal. A: Gen.* **1998**, *174*, 137.
(20) See Supporting Information for detailed information.
(21) Madon, R. J.; Boudart, M. *Ind. Eng. Chem. Fund.* **1982**, *21*, 438.
(22) Mukherjee, S.; Vannice, M. A. *J. Catal.* **2006**, *243*, 108.
(23) Van't Blik, H. F. J.; Van Zon, J. B. A. D.; Huizinga, T.; Vis, J. C.; Koningsberger, D. C.; Prins, R. *J. Am. Chem. Soc.* **1985**, *107*, 3139.
(24) (a) Van Hardeveld, R.; Hartog, F. *Surf. Sci.* **1969**, *15*, 189. (b) Veisz, B.; Király, Z.; Tóth, L.; Pécz, B. *Chem. Mater.* **2002**, *14*, 2882.
(25) TOF and TON reported herein are defined as TOF = (mol of H_2 consumed)/(total mol of Rh)/time; TON = (TOF) × (time). That is, the TOF and TON values reported are not corrected for the amount of surface metal atoms or the number of true active sites.
(26) Spivey, J. J. *Catalysis*: RSC, Cambridge, Vol. *16*, 2002.
(27) Rahaman, M. V.; Vannice, M. A. *J. Catal.* **1991**, *127*, 251.